



**HAL**  
open science

# Multiresolution Framework on the Interval based on Fibonacci Tiling, B-splines and Lifting Scheme

Cédric Gérot, Sylvain Meignen

► **To cite this version:**

Cédric Gérot, Sylvain Meignen. Multiresolution Framework on the Interval based on Fibonacci Tiling, B-splines and Lifting Scheme. [Research Report] GIPSA-lab. 2015. hal-01256233

**HAL Id: hal-01256233**

**<https://hal.science/hal-01256233>**

Submitted on 14 Jan 2016

**HAL** is a multi-disciplinary open access archive for the deposit and dissemination of scientific research documents, whether they are published or not. The documents may come from teaching and research institutions in France or abroad, or from public or private research centers.

L'archive ouverte pluridisciplinaire **HAL**, est destinée au dépôt et à la diffusion de documents scientifiques de niveau recherche, publiés ou non, émanant des établissements d'enseignement et de recherche français ou étrangers, des laboratoires publics ou privés.

# Multiresolution Framework on the Interval based on Fibonacci Tiling, B-splines and Lifting Scheme

Cédric Gérot

*Univ. Grenoble Alpes, GIPSA-Lab, F-38000 Grenoble, France  
CNRS, GIPSA-Lab, F-38000 Grenoble, France*

Sylvain Meignen

*Univ. Grenoble Alpes, LJK, F-38000 Grenoble, France  
CNRS, LJK, F-38000 Grenoble, France*

## Abstract

In this paper, we introduce a multiresolution analysis on the interval based on non-uniform B-splines defined on the Fibonacci tiling. The construction of the multiscale structure based on the substitution rules of an L-system allows the derivation of a known framework from the regular dyadic setting to a non-uniform setting while limiting the number of different filters to a few and keeping a similar stability. After having explained how our approach fits into a biorthogonal framework, we detail how to build analysis wavelet functions in the B-spline setting. Then the emphasis is put on the definition of boundary scaling and wavelet functions by means of scaling equations. Our implementation of the multiresolution structure is done in such a way that the computation is carried out in place. Finally, a numerical analysis of the stability of the proposed scheme shows its similar behavior to the same multiresolution analysis that would be derived on a dyadic sampling.

## 1 Introduction

Wavelets built on an irregular grid hierarchy are not translates and dilates of a single mother wavelet and lead to multiresolution transforms with, in the most general case, as many different rules as there are samples [Daubechies et al., 1999]. However it is possible to define an irregular grid hierarchy with a quasicrystal structure which allows us to define wavelets from a finite number of mother wavelets [Bernuau, 1998]. Andrieu *et al.* use substitution rules to define such a quasicrystal grid hierarchy and the associated semiorthogonal B-spline wavelets on the line with the aim to do a wavelet analysis of quasicrystal diffraction patterns [Andrieu et al., 2004]. With zero-degree B-spline basis functions, a full multiresolution framework can be implemented, but with higher degree basis functions, of the reconstruction and decomposition sides of the associated multiresolution framework, only the former can be efficiently implemented. Indeed, as explained by Lyche and Quak for their construction of B-spline wavelets on the interval, semiorthogonality makes the design of a good decomposition algorithm difficult [Lyche et al., 2001, Quak, 2002]. Since a direct computation of the inverse of the reconstruction leads to full matrices, the decomposition is rather applied by solving a linear system which can be different at each resolution. On the contrary, we want to decompose the signal using a finite number of localized filters. To do so, we drop semiorthogonality for general biorthogonality, which allows us to design non-uniform B-spline wavelets on a hierarchy of irregular grids defined by the substitution rules of Fibonacci L-system [Nivoliens et al., 2012], and associated with local linear decomposition and reconstruction making up a perfect reconstruction filter bank. Our construction, inspired by the designing of second generation wavelets with a lifting scheme [Sweldens, 1998], is made up of four successive steps presented in successive sections in this paper. In §2, we define a multiresolution analysis, i.e. a set of nested spaces spanned by scaling functions. In §3, we build a subdivision scheme from refinement

relations between scaling functions. In §4, we carry out in–place implementation of the perfect reconstruction filter bank based on the previously defined subdivision scheme. In §5, we stabilize the filter bank by means of extra *updating* elementary steps. Finally, since we aim to deal with data displayed on an interval, specific subdivision rules and update filters are defined at the interval boundaries in §6. Our construction can be viewed as the derivation of biorthogonal B–spline wavelets defined in the regular dyadic setting by Cohen Daubechies and Feauveau [Cohen et al., 1992] and their adaptations to the interval [Bittner, 2006, Primbs, 2010, Černá and Finěk, 2011] to a Fibonacci tiling on the interval, while keeping similar stability properties as shown by numerical experiments presented in §7.

## 2 Multiresolution Analysis

Let  $\mathcal{S}$  be a space of functions defined on a 1D–domain  $\Omega$ . A multiresolution analysis of  $\mathcal{S}$  is a sequence of closed subspaces  $\{V_j \subset \mathcal{S} \mid j \in \mathcal{J} \subset \mathbb{N}\}$  so that [Sweldens, 1998]:

1.  $V_j \subset V_{j+1}$ ,
2.  $\bigcup_{j \in \mathcal{J}} V_j$  is dense in  $\mathcal{S}$ ,
3. for each  $j \in \mathcal{J}$ ,  $V_j$  has a Riesz basis given by *scaling functions*  $\{\varphi_{j,\kappa} \mid \kappa \in \mathcal{K}(j)\}$ ,

where  $\mathcal{K}(j)$  is an index set satisfying  $\mathcal{K}(j) \subset \mathcal{K}(j+1)$ . When successive elements of  $\mathcal{K}(j)$  will be considered, we will name them  $\{t_{j,k} \mid k = 1, \dots, \#\mathcal{K}(j)\}$ .

In the *first generation wavelet* setting, scaling functions are translates and dilates of one *mother* scaling function. On the contrary, the *second generation wavelet* setting allows to deal with hierarchies of irregular grids without mother scaling function [Daubechies et al., 1999]. Our goal is to define a setting which is in–between, based on a hierarchy of irregular grids and where scaling functions are defined as translates and dilates of a small set of different functions.

We define the scaling functions  $\varphi_{j,\kappa}$  as non–uniform B–spline functions of order  $d+1$  (piecewise polynomial of degree  $d$ ) defined on  $d+1$  successive intervals  $[t_{j,k}, t_{j,k+1}]$ ,  $\dots$ ,  $[t_{j,k+d}, t_{j,k+d+1}]$  where  $\kappa = t_{j,k}$ , and normalized in the sense given in [de Boor, 1976]:

$$\varphi_{j,\kappa}(x) := \frac{t_{j,k+d+1} - t_{j,k}}{d+1} M_{t_{j,k}, \dots, t_{j,k+d+1}}(x),$$

where  $M_{t_{j,k}, \dots, t_{j,k+d+1}}(x) = (d+1)[t_{j,k}, \dots, t_{j,k+d+1}](\cdot - x)_+^d$  is the B–spline of Curry and Schoenberg,  $x_+^d = (\max\{0, x\})^d$  and  $[t_{j,k}, \dots, t_{j,k+d+1}]f$  denotes the  $(d+1)$ –th divided difference for the function  $f$  at the points  $\{t_{j,l}\}_{l=k}^{k+d+1}$ . In [de Boor, 1973], it is shown that  $\{\varphi_{j,\kappa} \mid \kappa \in \mathcal{K}(j)\}$ , is a Riesz basis in  $L_\infty$  of  $V_j$ . Note that if we were interested in other norms  $L_p$ ,  $1 \leq p \leq \infty$ , we could choose  $\left\{((d+1)/(t_{j,k+d+1} - t_{j,k}))^{1/p} \varphi_{j,\kappa}\right\}$  as a Riesz basis in  $L_p$  of  $V_j$ .

A sufficient condition for these scaling functions  $\varphi_{j,\kappa}$  to be defined as translates and dilates of a small set of functions is to impose any interval  $[t_{j,l}, t_{j,l+1}]$  to have its length in a set  $\{a_i^{(j)} = a_i/\rho^j, i \in I \subset \mathbb{N}\}$ , where  $\rho$  is a constant ratio and  $I$  a finite set. As shown in [Nivoliens et al., 2012], an L–system is a convenient tool to define such a set of intervals with a finite set of rules describing how to split each interval of length  $a_i^{(j)}$  into intervals of length  $a_i^{(j+1)}$ . An L–system is defined by a set of symbols  $\{A_i, i \in I\}$ , a set of rewriting rules

$$A_i \rightarrow A_{i_1} \dots A_{i_r}, \tag{2.1}$$

where  $(i_1, \dots, i_r) \in I^r$ , the  $r$  labels  $A_{i_1} \dots A_{i_r}$  being not necessarily different, and an axiom defined as an initial word of symbols. In [Nivoliens et al., 2012], such an L–system is said to be *valid* if there exist positive real numbers  $a_i$  and a ratio  $\rho$  strictly larger than 1 such that the rules (2.1) are compatible with the split of intervals with length  $a_i^{(j)}$ , that is  $a_i = \sum_{l=1}^r (a_{i_l}/\rho)$ . If the L–system is valid, then its rules define the subsets  $\mathcal{K}(j)$  and the subspaces  $V_j := \text{clos span}\{\varphi_{j,\kappa}, \kappa \in \mathcal{K}(j)\}$  define a multiresolution analysis of  $\mathcal{S} = L_\infty(\Omega)$ .

## 2.1 The case of Fibonacci L–system and cubic B–splines

In this article we consider the Fibonacci system which is defined by labels  $\{A_1 = L, A_2 = S\}$  and rules  $\{L \rightarrow LS, S \rightarrow L\}$ , with the following compatible lengths  $\{a_1 = 1, a_2 = 1/\phi\}$  and ratio  $\rho = \phi$ , where  $\phi = \frac{1+\sqrt{5}}{2} > 1$  is the golden number. An infinite word obtained using these rules with  $\{L\}$  as the axiom, is called the Fibonacci word which is known to contain only  $d + 2$  different subwords of length  $d + 1$ . This means that, in the case of cubic B–splines scaling functions, at each level  $j$ , scaling functions  $\varphi_{j,\kappa}$  are defined as dilates and translates of a set of five different B–splines whose support is made up of intervals labeled as  $LSLL$ ,  $SLLS$ ,  $LLSL$ ,  $LSL S$  or  $SLSL$ . The eleven other 4–length words, i.e. those containing  $SS$  (8) or  $LLL$  (3), cannot appear with the proposed rules and thus will never be present provided they are not in the axiom. The grid designed at each level  $j$  with such rules are sequences of intervals of length  $\phi^{-j}$ , labeled by  $L$  (for long), and intervals of length  $\phi^{-j-1}$ , labeled by  $S$  (for short). Let  $t_{j,k}$  be the  $k$ –th knot at level  $j$ ,  $\omega \in \{LSLL, SLLS, LLSL, LSL S, SLSL\}$  be the word defining the length of the support of the scaling function starting at  $\kappa = t_{j,k}$ , and  $j = 0$  be the coarsest level. The scaling functions may be written as:

$$\varphi_{j,\kappa}(x) = \varphi_\omega(\phi^j(x - t_{j,k})) = \frac{\text{len}(\omega)}{4} M_{\delta_{\omega,0}, \dots, \delta_{\omega,4}}(\phi^j(x - t_{j,k})), \quad (2.2)$$

where  $\delta_{\omega,l} := \phi^j(t_{j,k+l} - t_{j,k})$ , for  $l \in \{0, \dots, 4\}$ , and  $\text{len}(\omega) := \delta_{\omega,4} - \delta_{\omega,0} = \delta_{\omega,4}$  is the length of the support of  $\varphi_\omega$ :

$$\begin{cases} \text{len}(LSLL) = \text{len}(LLSL) = 3 + \phi^{-1}, \\ \text{len}(SLLS) = \text{len}(LSL S) = \text{len}(SLSL) = 2 + 2\phi^{-1}. \end{cases}$$

The five mother functions  $\varphi_\omega$  are shown in Figure 1.

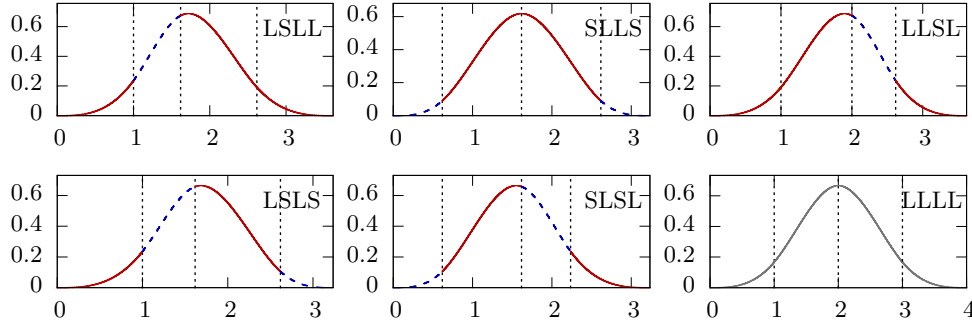


Figure 1: The five mother scaling functions  $\varphi_\omega$  with plain red parts defined above  $L$  intervals and blue dashed parts defined above  $S$  intervals. At the bottom right, the mother scaling function  $\varphi_{LLLL}$  used in the regular setting

Note that these scaling functions would have been those designed in [Andrle et al., 2004] if the authors had chosen their so–called minimal case of first category substitution rules instead of those of second category. They call Fibonacci chain a word produced by rules of whichever category. However, the case of  $\Omega$  being an interval is not considered in [Andrle et al., 2004], and requires to add extra boundary scaling functions. This particular case is handled in §6.

**Regular dyadic setting** The same modeling for the well-known regular dyadic case would define an L–system with one label  $L$ , one rule  $L \rightarrow LL$ , one length 1, a ratio  $\rho = 2$ , and one mother scaling function with a support labeled  $LLLL$  and  $\text{len}(LLLL) = 4$  shown at the bottom right in Figure 1.

### 3 Subdivision scheme

The subdivision scheme associated with these scaling functions was already defined in [Nivoliens et al., 2012]. Nevertheless let us recall the main steps of its definition. Let  $f \in V_j$  be defined as  $f(x) = \sum_{\kappa \in \mathcal{K}(j)} f_{j,\kappa} \varphi_{j,\kappa}(x)$ . Since  $V_j \subset V_{j+1}$ , there are  $\{f_{j+1,\kappa}, \kappa \in \mathcal{K}(j+1)\}$  such that  $f(x) = \sum_{\kappa \in \mathcal{K}(j+1)} f_{j+1,\kappa} \varphi_{j+1,\kappa}(x)$ . Stencils of the subdivision scheme associated with the scaling functions write coefficients  $f_{j+1,\kappa}$  as linear combination of coefficients  $f_{j,\kappa}$ .

Let  $p_{j,k}$  be the blossom of the polynomial piece of spline function  $f$  on  $[t_{j,k}, t_{j,k+1})$ , that is the  $d$  linear function (with values in  $\mathbb{R}$ ) such that  $p_{j,k}(t, \dots, t) = f(t)$  on  $[t_{j,k}, t_{j,k+1})$ . Then, as explained in [Goldman, 1990], we can write with  $\kappa = t_{j,k}$ ,

$$f_{j,\kappa} = p_{j,k}(t_{j,k+1}, \dots, t_{j,k+d}). \quad (3.1)$$

Note that for all  $m \in \{k, \dots, k+d\}$ ,  $p_{j,k}(t_{j,k+1}, \dots, t_{j,k+d}) = p_{j,m}(t_{j,k+1}, \dots, t_{j,k+d})$ , and if  $[t_{j+1,l}, t_{j+1,l+1}) \subset [t_{j,k}, t_{j,k+1})$ , then  $p_{j+1,l} = p_{j,k}$ . From (3.1) and the multilinearity of  $p_{j,k}$ , we deduce the subdivision stencils.

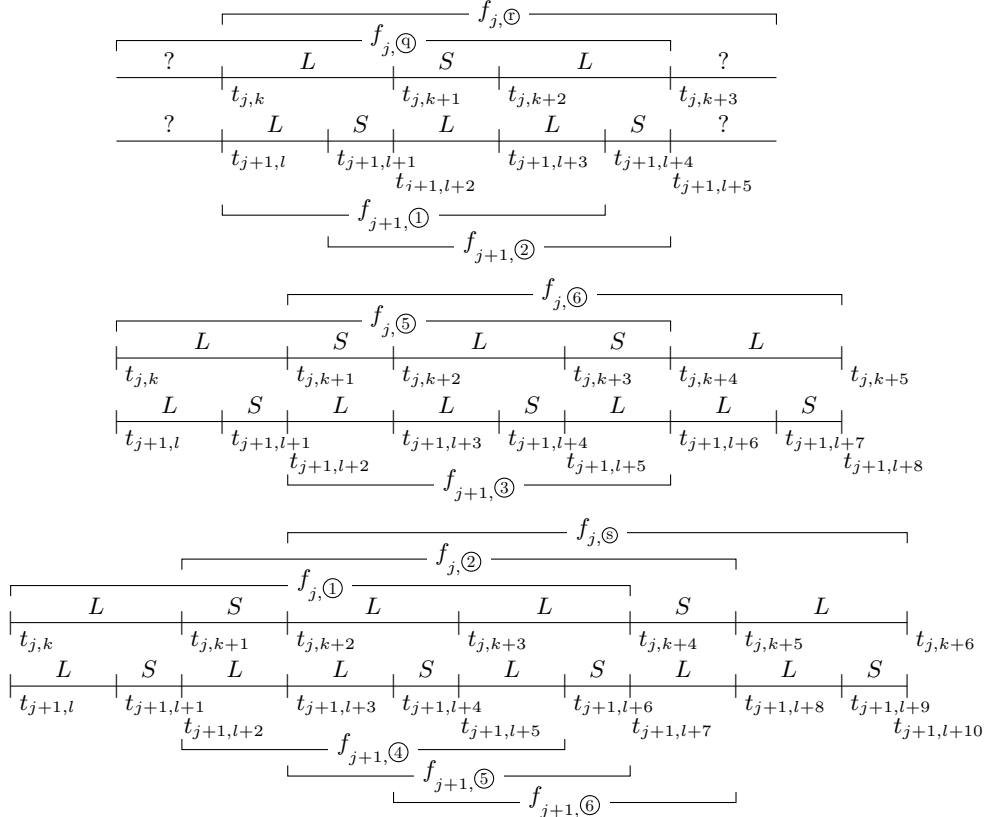


Figure 2: Configuration around the splitting of  $LSL$ ,  $SLS$  and  $LL$

Because neither  $SS$  nor  $LLL$  can be produced by the Fibonacci rules, only three configurations can occur, corresponding to the splitting of  $LSL$ ,  $SLS$ , and  $LL$  (Figure 2). These three configurations give birth to three sets of stencils (3.2) that depend on the kind of intervals making up the support of the associated functions. More precisely, six classes of coefficients can be defined and, for the sake of simplicity, we will sometimes write  $f_{j,\textcircled{\kappa}}$  with  $\textcircled{\kappa} \in \{\textcircled{1}, \dots, \textcircled{6}\}$  instead of  $f_{j,\kappa}$  with  $\kappa \in \mathcal{K}(j)$ , where  $f_{j,\textcircled{1}}$  is associated with  $\varphi_{LSLL}$ ,  $f_{j,\textcircled{2}}$  with  $\varphi_{SLLS}$ ,  $f_{j,\textcircled{3}}$  with  $\varphi_{LLSL}$  and the following scaling function is  $\varphi_{LSLL}$ ,  $f_{j,\textcircled{4}}$  with

$\varphi_{L L S L}$  and the following scaling function is  $\varphi_{L S L S}$ ,  $f_{j,\textcircled{5}}$  with  $\varphi_{L S L S}$ , and  $f_{j,\textcircled{6}}$  with  $\varphi_{S L S L}$ .

$$\begin{cases} f_{j+1,\textcircled{1}} &= (4 - 2\phi) f_{j,\textcircled{4}} + (2\phi - 3) f_{j,\textcircled{2}}, \\ f_{j+1,\textcircled{2}} &= (5 - 3\phi) f_{j,\textcircled{4}} + (3\phi - 4) f_{j,\textcircled{2}}, \\ f_{j+1,\textcircled{3}} &= \left(\frac{2\phi-1}{5}\right) f_{j,\textcircled{5}} + \left(\frac{6-2\phi}{5}\right) f_{j,\textcircled{6}}, \\ f_{j+1,\textcircled{4}} &= (7 - 4\phi) f_{j,\textcircled{1}} + (4\phi - 6) f_{j,\textcircled{2}}, \\ f_{j+1,\textcircled{5}} &= \left(\frac{18-11\phi}{2}\right) f_{j,\textcircled{1}} + (6\phi - 9) f_{j,\textcircled{2}} + \left(\frac{2-\phi}{2}\right) f_{j,\textcircled{3}}, \\ f_{j+1,\textcircled{6}} &= (2 - \phi) f_{j,\textcircled{2}} + (\phi - 1) f_{j,\textcircled{3}}, \end{cases} \quad (3.2)$$

with  $(\textcircled{4}, \textcircled{5}) \in \{(\textcircled{3}, \textcircled{1}), (\textcircled{4}, \textcircled{5}), (\textcircled{6}, \textcircled{1})\}$  and  $\textcircled{3} \in \{\textcircled{3}, \textcircled{4}\}$ . Let us detail the equations for one of the two stencils involved in the first configuration:

$$\begin{aligned} f_{j+1,\textcircled{1}} &= p_{j+1,l}(t_{j+1,l+1}, t_{j+1,l+2}, t_{j+1,l+3}) = p_{j,k}(t_{j+1,l+1}, t_{j,k+1}, t_{j,k+2}) \\ &= \frac{t_{j,k+3} - t_{j+1,l+1}}{t_{j,k+3} - t_{j,k}} p_{j,k}(t_{j,k}, t_{j,k+1}, t_{j,k+2}) \\ &\quad + \frac{t_{j+1,l+1} - t_{j,k}}{t_{j,k+3} - t_{j,k}} p_{j,k}(t_{j,k+1}, t_{j,k+2}, t_{j,k+3}) \\ &= \frac{1 + \phi + \phi^2}{2\phi^2 + \phi} f_{j,\textcircled{4}} + \frac{\phi}{2\phi^2 + \phi} f_{j,\textcircled{2}} = (4 - 2\phi) f_{j,\textcircled{4}} + (2\phi - 3) f_{j,\textcircled{2}}. \end{aligned}$$

The last equality comes from the equation satisfied by the golden ratio  $\phi^2 = \phi + 1$  which allows us to linearize powers of  $\phi$ . From these stencils and Figure 2, one can write the refinement relations satisfied by the scaling functions:

$$\begin{aligned} \varphi_{L S L L}(x) &= (2\phi - 3) \varphi_{L S L L}(\phi x) + (3\phi - 4) \varphi_{S L L S}(\phi x - 1) \\ &\quad + (7 - 4\phi) \varphi_{L L S L}(\phi x - 1 - \phi^{-1}) + \left(\frac{18-11\phi}{2}\right) \varphi_{L S L S}(\phi x - 2 - \phi^{-1}), \\ \varphi_{S L L S}(x) &= (4\phi - 6) \varphi_{L L S L}(\phi x) + (6\phi - 9) \varphi_{L S L S}(\phi x - 1) \\ &\quad + (2 - \phi) \varphi_{S L S L}(\phi x - 2), \\ \varphi_{L L S L}(x) &= \left(\frac{2-\phi}{2}\right) \varphi_{L S L S}(\phi x) + (\phi - 1) \varphi_{S L S L}(\phi x - 1) \\ &\quad + (4 - 2\phi) \varphi_{L S L L}(\phi x - 1 - \phi^{-1}) + (5 - 3\phi) \varphi_{S L L S}(\phi x - 2 - \phi^{-1}), \\ \varphi_{L S L S}(x) &= (2\phi - 3) \varphi_{L S L L}(\phi x) + (3\phi - 4) \varphi_{S L L S}(\phi x - 1) \\ &\quad + \left(\frac{2\phi-1}{5}\right) \varphi_{L S L S}(\phi x - 1 - \phi^{-1}), \\ \varphi_{S L S L}(x) &= \left(\frac{6-2\phi}{5}\right) \varphi_{S L S L}(\phi x) + (4 - 2\phi) \varphi_{L S L L}(\phi x - \phi^{-1}) \\ &\quad + (5 - 3\phi) \varphi_{S L L S}(\phi x - 1 - \phi^{-1}). \end{aligned} \quad (3.3)$$

## 4 Filter bank and wavelets

From here we do not construct semiorthogonal wavelets as proposed in [Bernuau, 1998, Andrieu et al., 2004]. Instead, we focus on the efficiency of the associated multiresolution framework that we want to be a perfect reconstruction filter bank with decomposition and reconstruction defined as simple local linear operators. The subdivision scheme may be implemented as part of a filter bank if the coefficients  $\{f_{j+1,\kappa}, \kappa \in \mathcal{K}(j+1)\}$  are split into two subsets: new coefficients introduced at level  $j+1$  called  $\mathcal{N}_j$  and initialized with zeros, and  $\mathcal{A}_j$  initialized with the coefficients at level  $j$  (in particular,  $\#\mathcal{A}_j = \#\mathcal{K}(j)$ ). We choose these subsets such that stencils (3.2) define short filters on  $\{f_{j+1,\kappa}, \kappa \in \mathcal{K}(j+1)\}$ : each coefficient  $f_{j,\kappa}$  is associated with the ‘‘central’’ knot  $t_{j,k+2}$  where  $\kappa = t_{j,k}$  and is changed into  $f_{j+1,\pi}$  where  $\pi = t_{j+1,p}$ , and such that  $t_{j,k+2} = t_{j+1,p+2}$ . The altered coefficients are  $f_{j+1,\textcircled{1}} \leftarrow f_{j,\textcircled{9}}$ ,  $f_{j+1,\textcircled{2}} \leftarrow f_{j,\textcircled{10}}$ , and  $f_{j+1,\textcircled{5}} \leftarrow f_{j,\textcircled{2}}$ . The new introduced coefficients are  $f_{j+1,\textcircled{3}}$ ,  $f_{j+1,\textcircled{4}}$  and  $f_{j+1,\textcircled{6}}$ . In order to be part of a filter bank implemented as a lifting scheme, the stencils should be decomposed into a succession of elementary steps, implemented *in place*. An elementary step is defined as follows:  $\{f_{j+1,\kappa}, \kappa \in \mathcal{K}(j+1)\}$  is partitioned into two subsets  $\mathcal{W}$  (read and written coefficients) and  $\mathcal{R}$  (read only coefficients). Each coefficient of  $\mathcal{W}$  is altered either by a multiplication with a non zero weight, or by an addition with a linear combination of coefficients of  $\mathcal{R}$ . The elementary steps composing a regular subdivision stencils, are typically defined with subsets  $(\mathcal{W}, \mathcal{R})$  being alternatively  $(\mathcal{N}_j, \mathcal{A}_j)$  and  $(\mathcal{A}_j, \mathcal{N}_j)$ . In our case, other subsets have to be used in order to deal with the configuration where no new coefficient is inserted between two successive coefficients. Let us present our choice for  $(\mathcal{W}, \mathcal{R})$  with the factorization of stencils into elementary steps corresponding to the subdivision of a sequence  $\{f_{j,\textcircled{5}}, f_{j,\textcircled{6}}, f_{j,\textcircled{1}}, f_{j,\textcircled{2}}, f_{j,\textcircled{9}}\}$ . This factorization is illustrated in Figure 3 where altered coefficients belonging to  $\mathcal{A}_j$  are drawn with black circles, new coefficients belonging to  $\mathcal{N}_j$  are drawn with white circles and, for each elementary step, coefficient belonging to  $\mathcal{W}$  are framed in a triangle. Weights are equal to:

$$\begin{cases} a_{35} = \frac{2\phi-1}{5}, \\ a_{36} = \frac{6-2\phi}{5}, \end{cases} \begin{cases} b_{11} = 4 - 2\phi, \\ b_{22} = \frac{\phi}{2}, \\ c_{12} = 10 - 6\phi, \\ d_{21} = 1 - \frac{\phi}{2}, \end{cases} \begin{cases} a_{41} = 7 - 4\phi, \\ a_{42} = 4\phi - 6, \\ a_{62} = 2 - \phi = b_{54}, \\ a_{6s} = \phi - 1 = b_{56}, \\ c_{55} = \frac{1}{2}. \end{cases}$$

This factorization is not unique and depends in particular on the order of the elementary steps that we apply. Let us detail it with the first two stencils of equation (3.2) where, in the case illustrated by Figure 3,  $(\textcircled{9}, \textcircled{10}) = (\textcircled{6}, \textcircled{1})$ .

$$\begin{cases} f_{j+1,\textcircled{1}} = b_{11} f_{j,\textcircled{6}} + c_{12} b_{22} f_{j,\textcircled{1}} = (4 - 2\phi) f_{j,\textcircled{6}} + (2\phi - 3) f_{j,\textcircled{1}}, \\ f_{j+1,\textcircled{2}} = d_{21} b_{11} f_{j+1,\textcircled{1}} + b_{22} f_{j,\textcircled{1}} = d_{21} b_{11} f_{j,\textcircled{6}} + (d_{21} c_{12} b_{22} + b_{22}) f_{j,\textcircled{1}} \\ = (5 - 3\phi) f_{j,\textcircled{6}} + (3\phi - 4) f_{j,\textcircled{1}}, \\ b_{11} = (4 - 2\phi), \\ d_{21} = (5 - 3\phi) / b_{11}, \\ b_{22} = (3\phi - 4) - d_{21} (2\phi - 3), \\ c_{12} = (2\phi - 3) / b_{22}. \end{cases}$$

From a practical point of view, when the filter bank is implemented *in place*, a unique vector of coefficients and zeros may be used. In order to apply the elementary steps described above, one should be able to find, in this vector, the first neighbors of a given coefficient within the same resolution  $j$ . Let  $J$  be the maximum resolution and  $\text{Fib}(j)$  be the Fibonacci sequence initialized with  $\text{Fib}(0) = \text{Fib}(1) = 1$ . Let  $\varphi_\omega$  be the mother function associated with the coefficient of interest. The left neighbor of this coefficient within the same resolution  $j$ , lies in the entry distanced by  $\text{Fib}(J - j + 1)$  if the second symbol of  $\omega$  is  $L$ , and  $\text{Fib}(J - j)$  if the symbol is  $S$ . The right neighbor is found similarly when considering the third

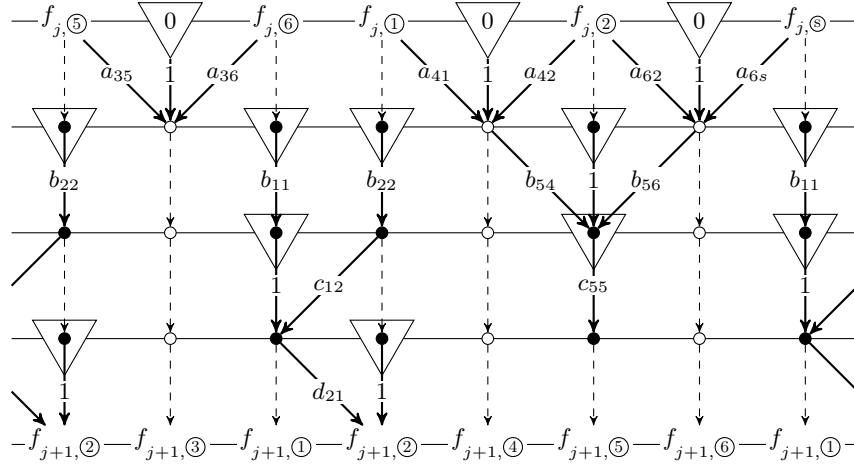


Figure 3: Subdivision stencils decomposed into *in place* steps

symbol of  $\omega$ . Note that in the regular dyadic setting, the distance between two coefficients of the same resolution  $j$  is  $2^{J-j}$ .

When a subdivision scheme can be decomposed into elementary steps, it is simple to invert it: elementary steps are applied in reversed order, with multiplicative update applied with inverse weights, and additive update applied with weights of opposite sign. From this it is straightforward to build a first multiresolution framework for signal decomposition and reconstruction as presented in [Sweldens, 1998, Schröder and Sweldens, 1995]. A signal at resolution  $j$  is a sequence of numbers  $\lambda_j := \{\lambda_{j,\kappa}\}_{\kappa \in \mathcal{K}(j)}$ . The framework is made up of a set of four operators for each resolution. A projection (or decimation) operator  $\tilde{H}_j: \lambda_j = \tilde{H}_j \lambda_{j+1}$  defines the signal at a coarser resolution. A prediction operator  $H_j^*$  reconstructs the fine signal with errors  $e_{j+1} := \lambda_{j+1} - H_j^* \lambda_j$ . Such an error signal takes non zero values on index set  $\mathcal{K}(j+1)$  but it can be coded into as a so-called *detail signal* indexed by  $\mathcal{M}(j) = \mathcal{K}(j+1) \setminus \mathcal{K}(j)$ :  $\gamma_j := \{\gamma_{j,m}\}_{m \in \mathcal{M}(j)}$ . This detail signal is defined from the fine signal with the operator  $\tilde{G}_j: \gamma_j = \tilde{G}_j \lambda_{j+1}$ . Finally an operator  $G_j^*$  constructs the error signal from the detail signal allowing us to write the perfect reconstruction as  $\lambda_{j+1} = H_j^* \lambda_j + G_j^* \gamma_j$ . These relationships are summarized in Figure 4 and equation (4.1).

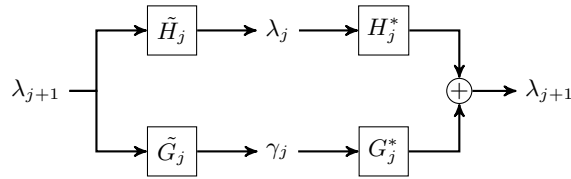


Figure 4: Filter bank for multiresolution analysis and synthesis

$$\begin{bmatrix} H_j^* & G_j^* \end{bmatrix} \begin{bmatrix} \tilde{H}_j \\ \tilde{G}_j \end{bmatrix} = H_j^* \tilde{H}_j + G_j^* \tilde{G}_j = I_{j+1}. \quad (4.1)$$

This notation is the one used in [Sweldens, 1998] with  $A^*$  being the adjoint of operator  $A$ . It highlights the fact that the prediction operator  $H_j^*$  defined using subdivision stencils, is the adjoint of a projection operator and vice versa.

Operators  $\tilde{H}_j$  and  $\tilde{G}_j$  constitute the *analysis* transform (named also *decomposition*) whereas operators  $H_j^*$  and  $G_j^*$  constitute the *synthesis* transform (or *reconstruction*). In order to get the so-called perfect reconstruction property, synthesis followed by analysis must be the identity as well, and the operators

must satisfy (4.2) where  $I_j$  is the identity operator for signals indexed by  $\mathcal{K}(j)$ .

$$\begin{bmatrix} \tilde{H}_j \\ \tilde{G}_j \end{bmatrix} \begin{bmatrix} H_j^* & G_j^* \end{bmatrix} = \begin{bmatrix} \tilde{H}_j H_j^* & \tilde{H}_j G_j^* \\ \tilde{G}_j H_j^* & \tilde{G}_j G_j^* \end{bmatrix} = \begin{bmatrix} I_j & 0 \\ 0 & I_j \end{bmatrix}. \quad (4.2)$$

When equations (4.1) and (4.2) are satisfied, the operators are said to be *biorthogonal*. The subdivision scheme designed in §3 defines a prediction operator  $H_j^*$ . The filter bank defined by its implementation into elementary steps as described in Figure 3 and its inverse, both applied to signals  $\lambda_j$  and  $\lambda_{j+1}$  instead of coefficients  $\{f_{j,\kappa}, \kappa \in \mathcal{K}(j)\}$  and  $\{f_{j+1,\kappa}, \kappa \in \mathcal{K}(j+1)\}$ , and with the coefficients of a detail signal  $\gamma_j$  replacing the zeros of  $\mathcal{N}_j$ , define such four biorthogonal operators.

For later purpose, we now translate the notation of operators  $H_j^*, G_j^*$  into the following linear equation:

$$\lambda_{j+1,\ell} = \sum_{\kappa \in \mathcal{K}(j)} h_{j,\kappa,\ell} \lambda_{j,\kappa} + \sum_{m \in \mathcal{M}(j)} g_{j,m,\ell} \gamma_{j,m}, \quad (4.3)$$

where  $h_{j,\kappa,\ell}$  are also involved into the refinement relations (3.3) satisfied by the non-uniform cubic B-spline scaling functions  $\varphi_{j,\kappa} = \sum_{\ell \in \mathcal{K}(j+1)} h_{j,\kappa,\ell} \varphi_{j+1,\ell}$ . Equation (4.3) defines also a basis of the complementary space  $W_j$  between two successive subspaces  $V_j \oplus W_j = V_{j+1}$  with wavelet functions  $\{\psi_{j,m}, m \in \mathcal{M}(j)\}$  defined as

$$\psi_{j,m} = \sum_{\ell \in \mathcal{K}(j+1)} g_{j,m,\ell} \varphi_{j+1,\ell}. \quad (4.4)$$

Like similar constructions, these first wavelets have poor properties and the whole framework can be improved by lifting [Sweldens, 1998, Schröder and Sweldens, 1995].

## 5 Update by lifting

Lifting means, as illustrated by Figure 5, adding another elementary step at the beginning of the synthesis filter bank decomposition described in Figure 3, where each detail coefficient  $\gamma_{j,m}$  (remember these occupy the zeros location on that figure) diffuses on samples in its vicinity. In order to keep the whole framework biorthogonal, the inverse of this update elementary step must be added at the end of the analysis filter bank. By doing so, one changes projection operator  $\tilde{H}_j$  and operator  $G_j^*$ , but not prediction operator  $H_j^*$  or operator  $\tilde{G}_j$ .

A biorthogonal framework with good properties is efficient, meaning made of short filters implemented *in place*, and stable, that is, allowing robust reconstruction and decomposition with respect to small value changes due to rounded computation (the golden ratio is an irrational number) or lossy transmission. Note that by construction the lifting structure of the filter bank ensures that the implementation can be done *in place*. The question of stability has been addressed carefully by Dahmen *et al.*, in particular in [Dahmen, 1994, Carnicer et al., 1996]. Ideally the condition numbers of transformation  $T$  relating the fine scale data to their multiscale representation and its inverse transform should remain uniformly bounded. This is equivalent to ask that the union of the basis functions of  $V_0$  and the wavelets at all levels constitute a Riesz basis of  $\mathcal{S}$ ; this is called *stability over all levels*. Necessary and sufficient conditions to get such a property are threefold: the analysis and synthesis transforms are uniformly bounded, they constitute a biorthogonal set of filters at each level, and the primal and dual subdivision schemes converge. If the set of filters are biorthogonal and the primal subdivision scheme converges by construction, to show that the dual non-uniform subdivision scheme converges is a difficult task.

To get stability over all levels another solution would be to define full orthogonal wavelet functions: the transformation  $T$  is then orthogonal. However, the construction of such orthogonal multiscale bases can lead to problematic inversion and are often associated with very large filters. To impose some kind of stability in a non orthogonal framework, a natural approximation is to keep the orthogonality between successive levels ( $W_j \perp V_j$ ) but to relax the orthogonality between wavelets at the same level; this is called

*semiorthogonality* [Quak, 2002, Bernuau, 1998, Andrlé et al., 2004]. As explained in the introduction, this is not satisfactory for our aim to keep a local approach and to define the wavelets with a finite number of different filters. To achieve this goal, a first solution consists in approximating semiorthogonality by defining wavelets basis functions in  $W_j$  that are orthogonal to only some functions in  $V_j$ . As summed up in [Maes and Bultheel, 2008], at this stage, two strategies to define the update are possible and these can be mixed: local semiorthogonal lifting [Lounsbery et al., 1997, Simoens and Vandewalle, 2003] and wavelets with vanishing moments [Sweldens, 1998]. As already noted in [Kobbelt and Schröder, 1998], each of these strategies leads to wavelets orthogonal to a different set of functions in  $V_j$ , being respectively a subset of the basis scaling functions  $\varphi_{j,k}$ , and some low degree polynomials. However, all sets of functions are not of equal importance for stability as first vanishing moment is considered as mandatory. Another solution consists in removing only one knot at each step as proposed by Bertram and then enforce a discrete orthogonalization instead of orthogonalization of continuous functions [Bertram, 2005]. We prefer to keep the possibility of removing several knots within each step, and choose consequently the solution based on the vanishing moments of wavelets. More precisely, we ask the wavelets to be orthogonal to  $x \mapsto x^p$ ,  $0 \leq p < \tilde{N}$ . Combination with local semiorthogonality is left for future work. Note that if dual wavelets existed, then they would be orthogonal to  $\{\varphi_{j,\kappa}\}$ , and so to  $x \mapsto x^p$ ,  $0 \leq p < N = d + 1 = 4$ .

**Regular dyadic setting** In the regular dyadic case, this modeling would yield to the Cohen–Daubechies–Feauveau  $(N, \tilde{N})$  biorthogonal wavelets [Cohen et al., 1992].

## 5.1 Wavelets as combination of fine scaling functions

Equation (4.4) enables us to write wavelets at level  $j$  as a combination of known B-spline scaling functions at level  $j + 1$ . As explained in [Sweldens and Schröder, 1996], the weights involved in such a refinement relation for a given  $\psi_{j,m}$ ,  $m \in \mathcal{M}(j)$ , can be obtained with our filter bank including the update step (Figure 5) by feeding the synthesis part of the filter bank with null values in every location except  $\gamma_{j,m} = 1$ . Then, the resulting signal  $\lambda_{j+1}$  contains the weights  $\{g_{j,m,l}, l \in \mathcal{K}(j + 1)\}$ . In order to satisfy the  $\tilde{N}$  equations corresponding to the expected  $\tilde{N}$  vanishing moments of wavelet functions, we use  $\tilde{N}$ -wide update filters. It follows that, as in the regular case [Cohen et al., 1992], the support of each wavelet  $\psi_{j,m}$  is made up with  $N + \tilde{N} - 1$  intervals at level  $j$ . This support is associated with a particular word  $\omega$  whose central symbol is always  $L$ , label of the interval whose splitting creates the detail coefficient  $\gamma_{j,m}$ . The labels of the support of the scaling functions involved in (4.4) are the subwords of length 4 of  $\omega$  after application of the  $L$ -system rules. Moreover, if the support begins at  $t_{j,k}$  then the wavelet can be written as

$$\psi_{j,m}(x) = \psi_{\omega}(\phi^j(x - t_{j,k})). \quad (5.1)$$

In the same line as what we did with classes of coefficients  $f_{j,\kappa}$ , we define classes of detail coefficients, but with the word  $\omega$  as subscript:  $\gamma_{j,\omega}$ .

In this section, we detail the case  $\tilde{N} = 2$ . Only three words of  $N + \tilde{N} - 1 = 5$  symbols with a central  $L$  are allowed in the word of Fibonacci, as containing neither  $SS$  nor  $LLL$ :  $LS-L-SL$ ,  $LS-L-LS$  and  $SL-L-SL$  (we emphasize the central  $L$ ). Therefore we define three classes of detail coefficients and one 2-wide update filter per class:  $[\alpha_{-1}, \alpha_{+1}]$  associated with  $\gamma_{j,LS-L-SL}$ ,  $[\beta_{-1}, \beta_{+1}]$  with  $\gamma_{j,LS-L-LS}$ , and  $[\nu_{-1}, \nu_{+1}]$  with  $\gamma_{j,SL-L-SL}$ . Using definition of mother scaling (2.2) and wavelet functions (5.1), as well as Figure 5, we write  $\psi_{j,LS-L-SL}$  as a combination of mother scaling functions associated with the five

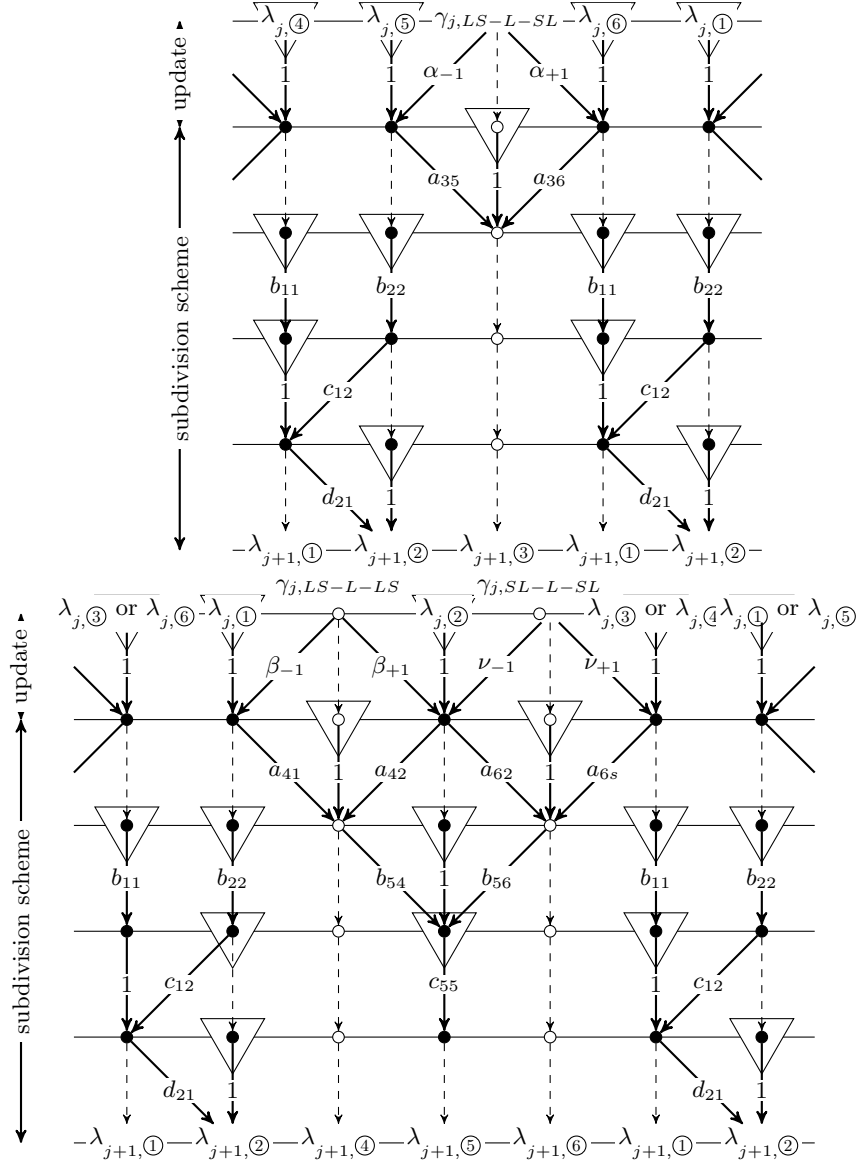


Figure 5: Lifting scheme for synthesis

4-length subwords of  $LSLLSLLS \leftarrow LSLSL$ :

$$\begin{aligned}
\psi_{LS-L-SL}(x) &= && [c_{12} \ b_{22} \ \alpha_{-1}] & \varphi_{LSLL}(\phi x) \\
&+ && [(1 + d_{21}c_{12}) \ b_{22} \ \alpha_{-1}] & \varphi_{SLLS}(\phi x - 1) \\
&+ && [1 + a_{35} \ \alpha_{-1} + a_{36} \ \alpha_{+1}] & \varphi_{LSSL}(\phi x - 1 - \phi^{-1}) \\
&+ && [b_{11} \ \alpha_{+1}] & \varphi_{LSLL}(\phi x - 2 - \phi^{-1}) \\
&+ && [d_{21} \ b_{11} \ \alpha_{+1}] & \varphi_{SLLS}(\phi x - 3 - \phi^{-1}) \\
&= && [(2\phi - 3) \ \alpha_{-1}] & \varphi_{LSLL}(\phi x) \\
&+ && [(3\phi - 4) \ \alpha_{-1}] & \varphi_{SLLS}(\phi x - 1) \\
&+ && \left[ 1 + \frac{2\phi-1}{5} \ \alpha_{-1} + \frac{6-2\phi}{5} \ \alpha_{+1} \right] & \varphi_{LSSL}(\phi x - 1 - \phi^{-1}) \\
&+ && [(4 - 2\phi) \ \alpha_{+1}] & \varphi_{LSLL}(\phi x - 2 - \phi^{-1}) \\
&+ && [(5 - 3\phi) \ \alpha_{+1}] & \varphi_{SLLS}(\phi x - 3 - \phi^{-1}).
\end{aligned} \tag{5.2}$$

Similarly, we write for the two other classes:

$$\begin{aligned}
\psi_{LS-L-S}(x) &= [(2\phi - 3) \beta_{-1}] \varphi_{LSLL}(\phi x) \\
&+ [(3\phi - 4) \beta_{-1}] \varphi_{SLLS}(\phi x - 1) \\
&+ [1 + (7 - 4\phi) \beta_{-1} + (4\phi - 6) \beta_{+1}] \varphi_{LSSL}(\phi x - 1 - \phi^{-1}) \\
&+ \left[ \frac{2-\phi}{2} + \frac{18-11\phi}{2} \beta_{-1} + (6\phi - 9) \beta_{+1} \right] \varphi_{LSLS}(\phi x - 2 - \phi^{-1}) \\
&+ [(2 - \phi) \beta_{+1}] \varphi_{SLSL}(\phi x - 3 - \phi^{-1}),
\end{aligned} \tag{5.3}$$

$$\begin{aligned}
\psi_{SL-L-SL}(x) &= [(4\phi - 6) \nu_{-1}] \varphi_{LSSL}(\phi x) \\
&+ \left[ \frac{\phi-1}{2} + (6\phi - 9) \nu_{-1} + \frac{2-\phi}{2} \nu_{+1} \right] \varphi_{LSLS}(\phi x - 1) \\
&+ [1 + (2 - \phi) \nu_{-1} + (\phi - 1) \nu_{+1}] \varphi_{SLSL}(\phi x - 2) \\
&+ [(4 - 2\phi) \nu_{+1}] \varphi_{LSLL}(\phi x - 2 - \phi^{-1}) \\
&+ [(5 - 3\phi) \nu_{+1}] \varphi_{SLLS}(\phi x - 3 - \phi^{-1}).
\end{aligned} \tag{5.4}$$

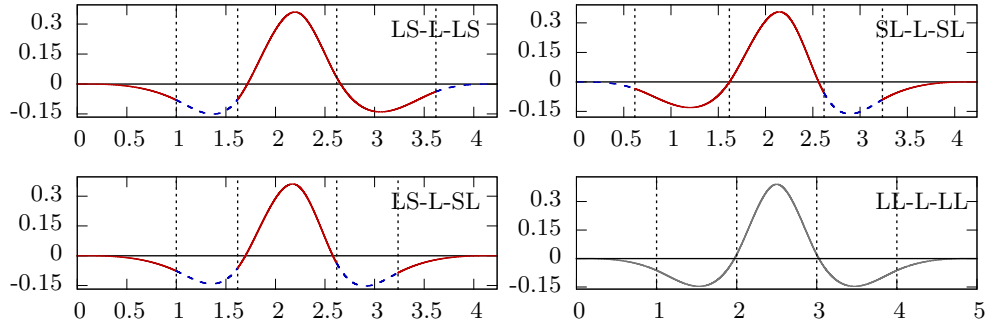


Figure 6: The three mother wavelet functions  $\psi_\omega$  for  $\tilde{N} = 2$  with plain red parts defined above  $L$  intervals and blue dashed parts defined above  $S$  intervals. At the bottom right, the mother wavelet function  $\psi_{LL-L-LL}$  used in the regular setting

## 5.2 Vanishing first moments of wavelets

As stated in [Neuman, 1981] for distinct knots and generalized in [de Boor, 1976] for  $t_{j,k} < t_{j,k+d+1}$  when B-splines of order  $d + 1$  are considered, the moments of the B-spline of Curry and Schoenberg  $M_{t_j, k, \dots, t_{j, k+d+1}}$  defined on the intervals between  $t_{j,k}$  and  $t_{j, k+d+1}$  with  $p \geq 0$  are:

$$\int x^p M_{t_j, k, \dots, t_{j, k+d+1}}(x) dx = \frac{(d+1)! p!}{(d+1+p)!} \sum_{k \leq k_1 \leq k_2 \leq \dots \leq k_p \leq k+d+1} t_{j, k_1} t_{j, k_2} \dots t_{j, k_p}.$$

In particular, the B-spline function  $\varphi_\omega$  defined by (2.2) satisfy

$$\int x^p \varphi_\omega(x) dx = \frac{\text{len}(\omega)}{4} \frac{4! p!}{(4+p)!} \mu_{\omega, p} \quad \text{with} \quad \mu_{\omega, p} := \sum_{0 \leq k_1 \leq k_2 \leq \dots \leq k_p \leq 4} \delta_{\omega, k_1} \delta_{\omega, k_2} \dots \delta_{\omega, k_p}.$$

As a consequence, with  $(l, s) \in \mathbb{Z}$ ,

$$\int x^p \varphi_\omega(\phi x - l - s\phi^{-1}) dx = \frac{\text{len}(\omega)}{4\phi^{p+1}} \sum_{r=0}^p \binom{p}{r} (l + s\phi^{-1})^{p-r} \frac{4! r!}{(4+r)!} \mu_{\omega, r}. \tag{5.5}$$

In particular for  $p = 0$ ,  $\mu_{\omega,0} = 1$  whatever  $\omega$ , and  $\int \varphi_{\omega}(\phi x - l - s\phi^{-1}) dx = \frac{\text{len}(\omega)}{4\phi}$  which leads to, with equations (5.2), (5.3): and (5.4):

$$\begin{aligned} 4\phi \int \psi_{LS-L-SL}(x) dx &= (2\phi + 2) \alpha_{-1} + (\phi + 2) + (2\phi + 2) \alpha_{+1}, \\ 4\phi \int \psi_{LS-L-LS}(x) dx &= (3\phi + 1) \beta_{-1} + (2\phi + 1) + (2\phi + 2) \beta_{+1}, \\ 4\phi \int \psi_{SL-L-SL}(x) dx &= (2\phi + 2) \nu_{-1} + (2\phi + 1) + (3\phi + 1) \nu_{+1}. \end{aligned}$$

From (5.1), first moment of  $\psi_{j,m}$  vanishes if first moment of the associated function  $\psi_{\omega}$  does and conditions for vanishing first moments of wavelets are:

$$\begin{cases} (\phi - 3) &= 2 \alpha_{-1} &+ 2 \alpha_{+1}, \\ \phi &= (1 - 2\phi) \beta_{-1} &- 2 \beta_{+1}, \\ \phi &= -2 \nu_{-1} &+ (1 - 2\phi) \nu_{+1}. \end{cases} \quad (5.6)$$

### 5.3 Vanishing second moments of wavelets

From (5.5), for any  $(l, s) \in \mathbb{Z}^2$ :

$$\int x \varphi_{\omega}(\phi x - l - s\phi^{-1}) dx = \frac{\text{len}(\omega)}{4\phi^2} (l + s\phi^{-1} + \frac{1}{5} \mu_{\omega,1}),$$

where  $\mu_{SLSL,1} = 6\phi - 2$ ,  $\mu_{LSLL,1} = 3\phi + 4$ ,  $\mu_{SLLS,1} = 5\phi$ ,  $\mu_{LLSL,1} = 2\phi + 6$ , and  $\mu_{LSLS,1} = 4\phi + 2$ . As a consequence,

$$\begin{aligned} 20\phi^2 \int x \psi_{LS-L-SL}(x) dx &= (32\phi + 20) \alpha_{-1} + (27\phi + 19) + (48\phi + 30) \alpha_{+1}, \\ 20\phi^2 \int x \psi_{LS-L-LS}(x) dx &= (37\phi + 24) \beta_{-1} + (34\phi + 21) + (50\phi + 30) \beta_{+1}, \\ 20\phi^2 \int x \psi_{SL-L-SL}(x) dx &= (30\phi + 20) \nu_{-1} + (32\phi + 19) + (53\phi + 31) \nu_{+1}. \end{aligned}$$

From (5.1), if first and second moments of  $\psi_{\omega}$  vanish, then second moment of  $\psi_{j,m}$  vanishes as well. With (5.6), we get the values of the update filters which make first and second moments of wavelets  $\psi_{j,m}$  vanish:

$$\begin{cases} \alpha_{-1} = 11 - 7\phi, & \left\{ \begin{array}{l} \beta_{-1} = \frac{2}{5}(4 - 3\phi), \\ \beta_{+1} = \frac{1}{2}(4 - 3\phi), \end{array} \right. & \left\{ \begin{array}{l} \nu_{-1} = \phi - 2, \\ \nu_{+1} = \phi - 2. \end{array} \right. \end{cases}$$

The three mother functions  $\psi_{\omega}$  are shown in Figure 6.

### 5.4 More vanishing moments of wavelets

With the same procedure, we can compute with our filter bank equations similar to (5.2), (5.3) and (5.4) for any width  $\tilde{N}$  of update filters. With (5.5) we can deduce equations similar to (5.6) for each power  $p \in \{0, \dots, \tilde{N} - 1\}$ , making up a linear system which can be solved numerically with a linear algebra library such as GSL. Update filters and resulting wavelet functions are available as supplementary materials linked from the main article webpage. Note that the number of different filters needed does not grow quickly with  $\tilde{N}$ : three filters are needed for  $\tilde{N} = 2$ , five filters for  $\tilde{N} = 4$  and seven filters for  $\tilde{N} \in \{6, 8\}$ .

## 6 Boundaries

In [Andrle, 2002, Andrle et al., 2004], the authors deal with infinite domain centered on the origin. With our Fibonacci L–system, they use these substitution rules, and so original functions, on the right side of the domain, while mirrored rules and functions are used on the left. A finite number of functions whose definition domain overlaps the two sides, remains possibly to be designed according to the chosen degree. The two extremities of the domain are not considered. Such a modeling is used to analyze quasicrystal diffraction patterns.

On the contrary, we want to design a framework which can be applied in practice and efficiently to signals defined on the interval, and the question of domain boundaries has to be handled. Different solutions can be investigated, either starting with adapting the framework filters as proposed in [Sweldens and Schröder, 1996], or defining new multiresolution spaces of functions living in the interval. We propose a solution which belongs to the second category. As what has been done by many authors to adapt uniform B–spline semiorthogonal [Chui and Quak, 1992] or biorthogonal [Bittner, 2006, Primbs, 2010, Černá and Finěk, 2011] wavelets to an interval, B–splines with multiple knots at endpoints of the interval may be introduced as a complement to *inner* ordinary B–spline scaling functions. Quak used also multiple knot B–splines as boundary scaling functions in his construction of semiorthogonal non–uniform B–spline wavelets [Quak, 2002]. Note that other adaptations of uniform B–spline wavelets to the interval preferred to define boundary scaling functions as combinations of truncated simple knot B–splines [Cohen et al., 1993, Dahmen et al., 1999].

### 6.1 L–system and scaling functions

We extend the framework described in the previous sections by adding to the Fibonacci L–system a new label  $X$  associated with the rule  $X \rightarrow X$  and a length equal to zero. Besides, the axiom  $\omega_0$  becomes  $X^d \omega_0 X^d$ , with B–splines of order  $d + 1$ . In our case,  $d = 3$  and we choose  $\omega_0 = L$ . If  $\omega_j$  is the word of symbols of the intervals after  $j$  subdivision steps with the previous framework,  $\omega_j$  is a subword of Fibonacci, meaning that  $\omega_{j+1} = \omega_{j-1} \omega_j$ . The word of symbols in the new framework after  $j$  steps is  $X^d \omega_j X^d$  and the number of samples in resolution  $j$  is equal to  $3 + \text{Fib}(j + 1)$ . Note that in the regular dyadic setting, this number of samples is equal to  $3 + 2^j$ .

Regarding scaling functions, since the first word is  $X^3 L X^3$ , four scaling functions are used in the first resolution  $j = 0$ :  $\varphi_{XXXL}$ ,  $\varphi_{XXLX}$ ,  $\varphi_{XLXX}$  and  $\varphi_{LXXX}$  shown in Figure 7 (top–left function, rightest function in the second row and the two first functions in the last row). The second word is  $X^3 L S X^3$ , defining five mother scaling functions for resolution  $j = 1$ :  $\varphi_{XXXL}$ ,  $\varphi_{XXLS}$ ,  $\varphi_{XLSX}$ ,  $\varphi_{LSXX}$ , and  $\varphi_{SXXX}$  shown in Figure 7 (the two first functions in the first row, the two last functions in the second row and the last function in the bottom row).

For  $j > 1$ , the word  $\omega_j$  starts always as  $X^3 L S L \dots$ , yielding to the three functions in the first row in Figure 7 as the first mother scaling functions used near the left boundary. However, the word  $\omega_j$  finishes alternatively as  $\dots L S L X^3$  or  $\dots L L S X^3$ : in even resolution  $j$ , the mother scaling functions shown in the second row in Figure 7 will be used near the right boundary, whereas for odd  $j$  the functions in the third row will be chosen. In total, twelve new mother scaling functions are introduced for managing boundaries.

Let us illustrate how the blossom–based construction of subdivision stencils presented in §3, adapts to such 0–length knot intervals. With the same notation, we can write (Figure 8):

$$\begin{aligned}
 f_{j+1,t_{j+1},0} &= p_{j+1,0}(t_{j+1,1}, t_{j+1,2}, t_{j+1,3}) = p_{j,0}(t_{j,1}, t_{j,2}, t_{j,3}) = f_{j,t_{j,0}}, \\
 f_{j+1,t_{j+1},1} &= p_{j+1,1}(t_{j+1,2}, t_{j+1,3}, t_{j+1,4}) = p_{j,1}(t_{j,2}, t_{j,3}, t_{j+1,4}) \\
 &= \frac{t_{j,4} - t_{j+1,4}}{t_{j,4} - t_{j,1}} p_{j,1}(t_{j,1}, t_{j,2}, t_{j,3}) + \frac{t_{j+1,4} - t_{j,1}}{t_{j,4} - t_{j,1}} p_{j,1}(t_{j,2}, t_{j,3}, t_{j,4}) \\
 &= \frac{1}{\phi^2} f_{j,t_{j,0}} + \frac{\phi}{\phi^2} f_{j,t_{j,1}} = (2 - \phi) f_{j,t_{j,0}} + (\phi - 1) f_{j,t_{j,1}}.
 \end{aligned}$$

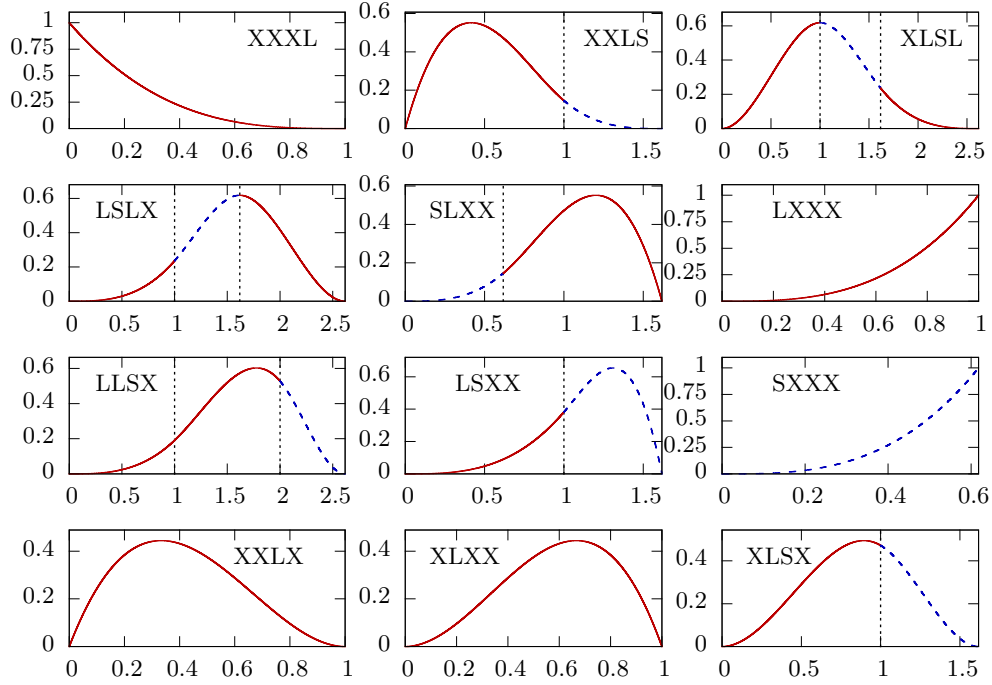


Figure 7: The twelve mother scaling functions  $\varphi_\omega$  with plain red parts defined above  $L$  intervals and blue dashed parts defined above  $S$  intervals, used near the boundaries with  $\tilde{N} = 2$ .

## 6.2 Update filters and wavelet functions

We follow the same process as the one described in previous sections, leading to filter banks implemented in place and wavelets with vanishing moments. Figures 8, 9, and 11 illustrate the synthesis filter banks for the different boundary neighborhoods considered above, and with an update elementary step designed in order to get wavelet functions with two vanishing moments. Note that for simplicity, we name in these figures the introduced classes of coefficients and details as  $\lambda_{j,\omega}$  instead of  $\lambda_{j,\textcircled{\omega}}$ . The associated wavelet functions satisfy the following equations, and are illustrated in Figure 10:

$$\begin{aligned}
\psi_{XX-L-SL}(x) &= (6 - 4\phi) \varphi_{XXLS}(\phi x) + (4\phi - 6) \varphi_{XLSL}(\phi x) \\
&\quad + (16\phi - 26) \varphi_{LSLL}(\phi x) + (21\phi - 34) \varphi_{SLLS}(\phi x - 1) \\
\psi_{LS-L-XX}(x) &= (21\phi - 34) \varphi_{LSLL}(\phi x) + (29\phi - 47) \varphi_{SLLS}(\phi x - 1) \\
&\quad + (7\phi - 11) \varphi_{LLSX}(\phi x - 1 - \phi^{-1}) \\
&\quad + (11 - 7\phi) \varphi_{LSXX}(\phi x - 2 - \phi^{-1}) \\
\psi_{SL-L-SX}(x) &= \frac{3-2\phi}{2} \varphi_{LLSL}(\phi x) + \frac{10-5\phi}{4} \varphi_{SLSL}(\phi x - 2) \\
&\quad + \frac{4-3\phi}{2} \varphi_{LSLX}(\phi x - 2 - \phi^{-1}) \\
\psi_{XX-L-XX}(x) &= (3 - 2\phi) \varphi_{XXLS}(\phi x) + (4\phi - 6) \varphi_{XLSX}(\phi x) \\
&\quad + (3 - 2\phi) \varphi_{LSXX}(\phi x) \\
\psi_{XX-L-SX}(x) &= (\phi - 2) \varphi_{XXLS}(\phi x) + (4\phi - 6) \varphi_{XLSL}(\phi x) \\
&\quad + (3 - 2\phi) \varphi_{LSLX}(\phi x)
\end{aligned}$$

On the contrary with wavelets defined far from the boundaries, these wavelet functions are not defined as the sum of five scaling functions. Indeed, due to the presence of  $X$  in the label of the support of the wavelet function, the word produced by the  $L$ -system rules contains less than five 4-length factors. For example,  $XXLSL \rightarrow XXLSLLS$  contains only four 4-length factors.

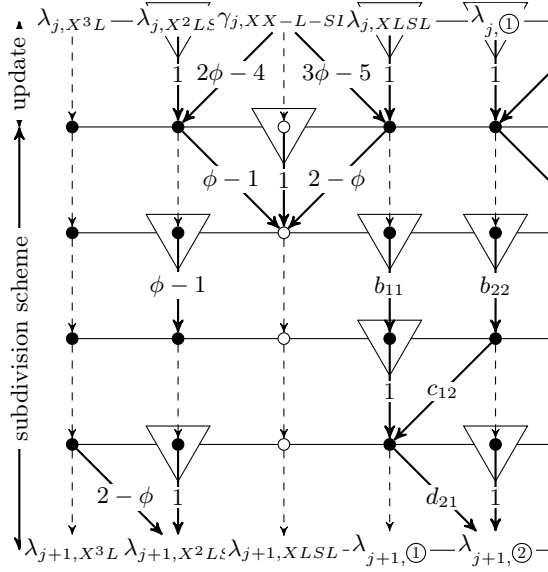


Figure 8: Lifting scheme for synthesis near the left boundary for  $j > 1$

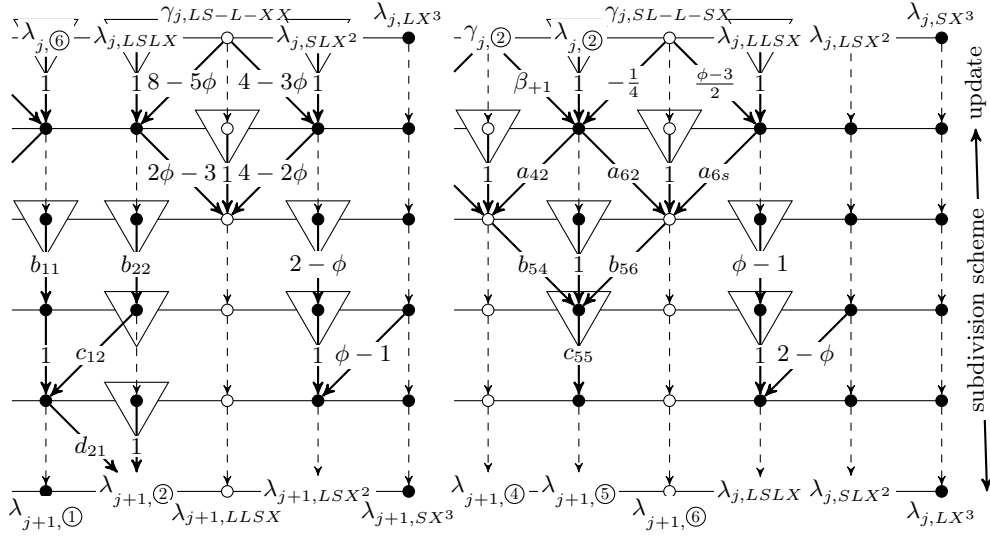


Figure 9: Lifting scheme for synthesis near the right boundary for  $j > 1$  and even (to the left) or odd (to the right)

The same procedure can be applied to design update filters defining wavelet functions with  $\tilde{N} > 2$  vanishing moments. However, as the filter width grows with  $\tilde{N}$ , the level must be greater than the minimum level which provides enough neighbors (for instance  $j \geq 2$  if  $\tilde{N} = 6$ ), and precautions have to be taken near the boundaries. If  $\tilde{N} \geq 6$ , some filters may not expand equally on the left and on the right of the *central*  $L$  interval. We choose to keep the filter width as short as possible and use the first following right neighbors to replace the neighbors which do not exist on the left, and vice versa near the right boundary of  $\Omega$ . This choice implies that several wavelet functions, such as  $\psi_{XXX-L-SLLSLSL}$  and  $\psi_{XXXLS-L-LSLSL}$ , may be defined as a linear combination of the same scaling functions. But due to the different position of the *central*  $L$  within the common  $\omega$ , these functions are well distinct. Note that, due to the presence of  $S$  intervals, these cases are less numerous in the Fibonacci setting than in the regular dyadic setting: they occur only for  $\tilde{N} \geq 8$  with only two wavelet functions per boundary defined with the same scaling functions within each level. In the regular dyadic setting, this occurs from  $\tilde{N} = 6$ , with  $\tilde{N}/2 - 1$  wavelet functions per boundary (in general,  $(\tilde{N} - N)/2 + 1$ ). Update filters for  $\tilde{N} \in \{4, 6, 8\}$  are

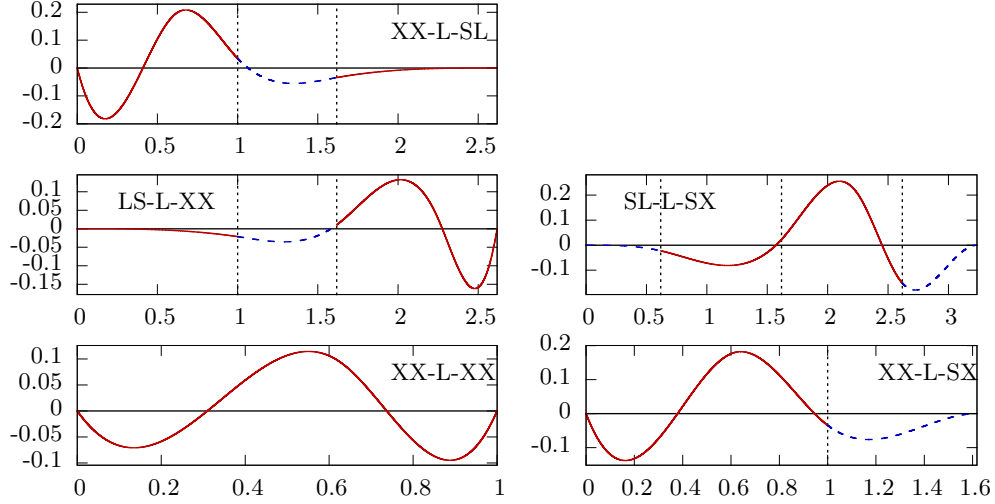


Figure 10: The five mother wavelet functions  $\psi_\omega$  used near boundaries, for  $\tilde{N} = 2$ , with plain red parts defined above  $L$  intervals and blue dashed parts defined above  $S$  intervals.

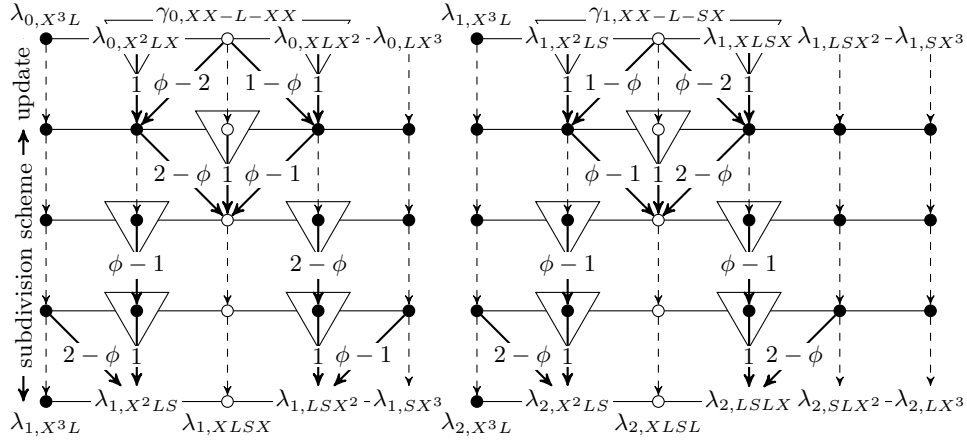


Figure 11: Lifting scheme for synthesis from  $j = 0$  to 1 (to the left) or from  $j = 1$  to 2 (to the right)

available as supplementary materials linked from the main article webpage.

**Regular dyadic setting** In the regular dyadic case, our construction to deal with boundaries would yield to the same wavelet functions as Type A wavelets built by Kai Bittner [Bittner, 2006].

## 7 Stability

In §5, we recalled the necessity for our multiresolution framework to be as stable as possible, with the desirable property of *stability over all levels* being subordinate to the convergence of the dual subdivision scheme, which is difficult to prove since the scheme is non-stationary. In this section, we give an insight into this stability through numerical analysis of condition number of the framework. But first of all, we remark that our framework fulfills the conditions for a weaker definition of stability proposed in [Carnicer et al., 1996]: the *uniform stability* of  $\{\Phi_j \cup \Psi_j\}$ , with  $\Phi_j := \{\tilde{\varphi}_{j,\kappa}, \kappa \in \mathcal{K}(j)\}$  and  $\Psi_j := \{\psi_{j,m}, m \in \mathcal{M}(j)\}$ .

## 7.1 Uniform stability

Let  $A_j$  be the synthesis operator from  $\mathcal{K}(j+1)$  onto  $\mathcal{K}(j+1)$  which transforms  $\lambda_j \cup \gamma_j$  into  $\lambda_{j+1}$  and  $B_j$  the analysis operator which, by construction, is the inverse of  $A_j$ . The sets  $\Phi_j$  and  $\Psi_j$  satisfy the hypotheses of Corollary 2.1 in [Carnicer et al., 1996], and then  $\{\Phi_j \cup \Psi_j\}$  is said *uniformly stable* if and only if

$$\|A_j\| = \mathcal{O}(1), \|B_j\| = \mathcal{O}(1), j \rightarrow \infty.$$

Whatever the update filter chosen in order to get wavelets with vanishing moments, there is only a finite number of different rules to be applied. Let us consider the norm of the operators defined by the infinity norm of their matrix representation which will be noted also as  $A_j$  and  $B_j$  for simplicity. The weights included in each line of  $A_j$  or  $B_j$  depend on a factor of a given length  $l$  in  $X^d \omega_j X^d$ . As we know that the number of different factors of length  $l$  in the infinite word of Fibonacci is  $l+1$  and because  $l$  does not depend on  $j$ , the number of different possible absolute row sums in  $A_j$  or  $B_j$  is finite, which leads to the result.

To be more specific, numerical experiments give  $\|A_j\|_\infty \approx 2$  and  $\|B_j\|_\infty \approx 4$  whatever  $\tilde{N}$ , yielding to a condition number  $\|A_j\|_\infty \cdot \|B_j\|_\infty < 10$  for any resolution  $j$  which is large enough (greater than 1 to 6, depending on  $\tilde{N} \in \{0, 2, 4, 6, 8\}$ ). Indeed,  $\omega_{j+1} = \omega_{j-1} \omega_j$  means that once  $\omega_{j_0}$  contains all the possible factors (without  $X$ ) of a given length, the following  $\omega_j$  do so. Moreover, the  $l$ -length factors starting with an  $X$  are the same whatever  $j$  as soon as  $3 + \text{Fib}(j+1) \geq l$ , when the  $l$ -length factors ending with  $X$  are the same every two resolutions.

Note that the boundary management does not alter too much this one-step stability. Indeed, if we compute the maximum absolute value row sum of  $B_j$  and  $A_j$  without the rows which contains a weight defined for the boundary management, the norms remain of the same order. Besides, these values are similar to the norms computed with similar frameworks designed with the regular dyadic hierarchy instead of the Fibonacci tiling.

## 7.2 Stability over all levels

The *stability over all levels* defined in [Carnicer et al., 1996] is closely related to the condition of the framework defined as follows. Let  $T_j$  be the synthesis operator from  $\mathcal{K}(j+1)$  onto  $\mathcal{K}(j+1)$  which transforms  $\lambda_0 \cup \bigcup_{k=0}^j \gamma_k$  into  $\lambda_{j+1}$ . The operators  $T_j$  are well conditioned if

$$\|T_j\| = \mathcal{O}(1), \|T_j^{-1}\| = \mathcal{O}(1), j \rightarrow \infty.$$

As for  $A_j$  and  $B_j$ , the weights in any row of  $T_j$  or  $T_j^{-1}$  are determined by a factor of a given length  $l_j$  in  $X^d \omega_j X^d$ . Unfortunately, in contrast with  $l$ , the length  $l_j$  grows with  $j$ , which prevents us to conclude to the stability over all levels. However, numerical experiments show that this instability is of the same order as the instability of the framework designed with the regular dyadic setting.

Let  $T_{j_0, \Delta}$  be the synthesis matrix which transforms  $\lambda_{j_0} \cup \bigcup_{k=j_0}^{j_0+\Delta} \gamma_k$  into  $\lambda_{j_0+\Delta}$ .  $T_{j_0, \Delta}^{-1}$  is the analysis matrix. Figure 12 (top left) shows the values of the condition number against  $\Delta$ , for different update lifting corresponding to  $\tilde{N} \in \{0, 2, 4, 6, 8\}$ , and with  $j_0 = 3$  which is the first level where the update filters for  $\tilde{N} = 8$  can be applied. As expected, the framework is more stable as  $\tilde{N}$  grows. However the condition numbers for  $\tilde{N} = 8$  are slightly higher than for  $\tilde{N} = 6$ . This counter-intuitive order appears with the rules added for managing the boundaries. Indeed, let us note  $\overline{T_{j_0, \Delta}}$  and  $\overline{T_{j_0, \Delta}^{-1}}$  the matrices without the rows containing at least one entry which depends on the boundary management. Note that the one is not the inverse of the other. However, with the same argument as the one used for the uniform stability, when  $j_0$  becomes large enough for these submatrices to contain all the possible set of weights within a row, their infinity norms are also the norms of the bi-infinite matrices corresponding to the framework applied on signals without boundary. Figure 12 (top right) shows the conditions numbers of these matrices with  $j_0 = 6$  which yields to norms numerically stable against  $j \geq j_0$ , whatever  $\tilde{N}$  and  $\Delta$ . The same general

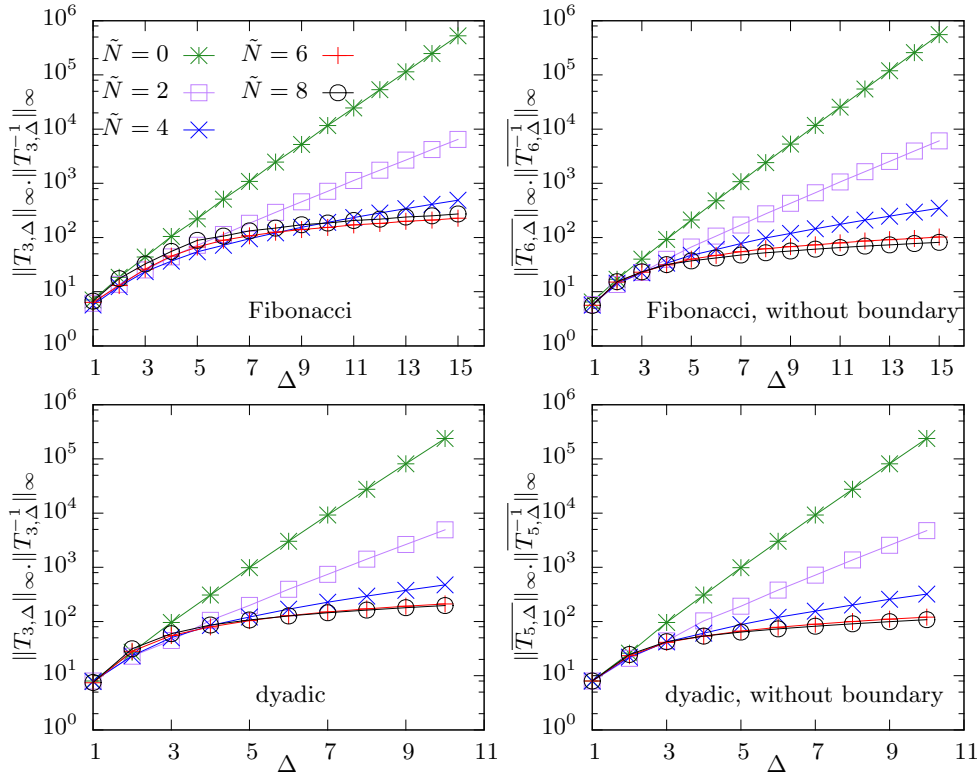


Figure 12: Condition numbers of  $\Delta$  successive steps of our Fibonacci framework (top row) and of the similar framework with the regular dyadic setting (bottom row), for  $\tilde{N} \in \{0, 2, 4, 6, 8\}$ . On the left, the norms are computed with all the rows. On the right, rows depending on the boundary management are excluded.

behavior of the condition numbers can be observed with, this time, the curve corresponding to  $\tilde{N} = 8$  strictly below the curve for  $\tilde{N} = 6$  for  $\Delta \geq 5$ .

The bottom row of the same figure shows the same quantities computed with the framework designed with the regular dyadic setting, and values for  $j_0$  and  $\Delta$  chosen in order to get similar numbers of samples at the finest resolution to those got in the experiments illustrated in the top row. The behavior and values of the quantities are very similar between the two rows. This can be explained by the low discrepancy between interval lengths of our non-uniform tiling, outside the boundaries neighborhood: within each resolution, the ratio between interval lengths is never greater than the golden ratio (1.618...).

## 8 Conclusion

In this paper, we have presented a new multiresolution analysis based on non uniform B-splines and defined on the Fibonacci grid. Similar constructions are possible with other valid L-system than Fibonacci substitution rules as far as the associated subdivision scheme can be decomposed into elementary steps. Define conditions on the L-system for such a decomposition to be possible is left for future work. Since we focus on the study of a signal supported on an interval, after having explained how to perform its decomposition at inner locations, the emphasis is put on the definition of boundary wavelets and scaling functions. In our framework, the analysis/synthesis steps are naturally associated with biorthogonal filters which allow the decomposition to be computed in place. Furthermore, since the downsampling rate between each level of resolution is lower than 2 and the filter bank is designed on non-uniform samples, we believe that the proposed decomposition could have good properties for further applications in particular in regard to aliasing. This aspect will be the scope of future work. Moreover, the analysis could be extended to image decomposition using a tensor-product approach and the properties of such an encoding

should be investigated. Finally, we carried a numerical study showing that the proposed multiscale representation is as stable as the same analysis implemented on a dyadic grid. Alternative strategies combining vanishing moments and local semiorthogonalization could improve the condition number of the framework [Simoens and Vandewalle, 2003]. Furthermore, the stability of the decomposition is not theoretically guaranteed yet, because the existence of the dual bases remains to be proven. However the lifting structure of the framework makes the first step of this study, that is, the definition of the dual non-stationary subdivision scheme, easier. But the proof of its convergence is a much more difficult task.

## References

- [Andrle, 2002] Andrle, M. (2002). *Ensembles modèles et analyse en ondelettes adaptées*. PhD thesis, Paris 7.
- [Andrle et al., 2004] Andrle, M., Burdík, C., and Gazeau, J.-P. (2004). Bernuau spline wavelets and sturmian sequences. *Journal of Fourier Analysis and Applications*, 10(3):269–300.
- [Bernuau, 1998] Bernuau, G. (1998). Wavelets bases adapted to a self-similar quasicrystal. *Journal of Mathematical Physics*, 39(8):4213–4225.
- [Bertram, 2005] Bertram, M. (2005). Single-knot wavelets for non-uniform B-splines. *Computer Aided Geometric Design*, 22(9):849–864.
- [Bittner, 2006] Bittner, K. (2006). Biorthogonal spline wavelets on the interval. In Chen, G. and Lai, M., editors, *Wavelets and Splines: Athens 2005, Mod. Methods Math.*, pages 93–104. Nashboro Press.
- [Carnicer et al., 1996] Carnicer, J. M., Dahmen, W., and Peña, J. M. (1996). Local decomposition of refinable spaces and wavelets. *Applied and Computational Harmonic Analysis*, 3(2):127–153.
- [Chui and Quak, 1992] Chui, C. K. and Quak, E. (1992). Wavelets on a bounded interval. In Braess, D. and Schumaker, L. L., editors, *Numerical Methods in Approximation Theory, Vol. 9*, volume 105 of *ISNM 105: International Series of Numerical Mathematics*, pages 53–75. Birkhuser Basel.
- [Cohen et al., 1992] Cohen, A., Daubechies, I., and Feauveau, J.-C. (1992). Biorthogonal bases of compactly supported wavelets. *Communications on Pure and Applied Mathematics*, 45(5):485–560.
- [Cohen et al., 1993] Cohen, A., Daubechies, I., and Vial, P. (1993). Wavelets on the interval and fast wavelet transforms. *Applied and Computational Harmonic Analysis*, 1(1):54–81.
- [Dahmen, 1994] Dahmen, W. (1994). Some remarks on multiscale transformations, stability and biorthogonality. In Laurent, P.-J., Le Méhauté, A., and Schumaker, L. L., editors, *Wavelets, Images and Surface Fitting, Curves and Surfaces II*, pages 157–188. A K Peters, Wellesley MT.
- [Dahmen et al., 1999] Dahmen, W., Kunoth, A., and Urban, K. (1999). Biorthogonal spline wavelets on the interval-stability and moment conditions. *Applied and Computational Harmonic Analysis*, 6(2):132–196.
- [Daubechies et al., 1999] Daubechies, I., Guskov, I., Schröder, P., and Sweldens, W. (1999). Wavelets on irregular point sets. *Phil. Trans. R. Soc. Lond. A*, 357(1760):2397–2413.
- [de Boor, 1973] de Boor, C. (1973). The quasi-interpolant as a tool in elementary polynomial spline theory. In Lorentz, G. G., Berens, H., Cheney, E. W., and Schumaker, L. L., editors, *Approximation theory*, pages 269–276. Academic Press, New York.

- [de Boor, 1976] de Boor, C. (1976). Splines as linear combinations of B-splines. a survey. In Lorentz, G. G., Chui, C. K., and Schumaker, L. L., editors, *Approximation theory II*, pages 1–47. Academic Press, New York.
- [Goldman, 1990] Goldman, R. N. (1990). Blossoming and knot insertion algorithms for B-spline curves. *Computer Aided Geometric Design*, 7(1-4):69–81.
- [Kobbelt and Schröder, 1998] Kobbelt, L. and Schröder, P. (1998). A multiresolution framework for variational subdivision. *ACM Trans. Graph.*, 17(4):209–237.
- [Lounsbery et al., 1997] Lounsbery, M., DeRose, T. D., and Warren, J. (1997). Multiresolution analysis for surfaces of arbitrary topological type. *ACM Trans. Graph.*, 16(1):34–73.
- [Lyche et al., 2001] Lyche, T., Mørken, K., and Quak, E. (2001). Theory and algorithms for nonuniform spline wavelets. In Dyn, N., Leviatan, D., Levin, D., and Pinkus, A., editors, *Multivariate Approximation and Applications*, pages 152–187. Cambridge University Press.
- [Maes and Bultheel, 2008] Maes, J. and Bultheel, A. (2008). Stability analysis of biorthogonal multiwavelets whose duals are not in and its application to local semiorthogonal lifting. *Applied Numerical Mathematics*, 58(8):1186–1211.
- [Neuman, 1981] Neuman, E. (1981). Moments and Fourier transforms of B-splines. *Journal of Computational and Applied Mathematics*, 7(1):51–62.
- [Nivoliers et al., 2012] Nivoliers, V., Gérot, C., Ostromoukhov, V., and Stewart, N. F. (2012). L-system specification of knot-insertion rules for non-uniform B-spline subdivision. *Computer Aided Geometric Design*, 29(2):150–161.
- [Primbs, 2010] Primbs, M. (2010). New stable biorthogonal spline-wavelets on the interval. *Results in Mathematics*, 57(1-2):121–162.
- [Quak, 2002] Quak, E. (2002). Nonuniform B-splines and B-wavelets. In Iske, A., Quak, E., and Floater, M. S., editors, *Tutorials on Multiresolution in Geometric Modelling*, Mathematics and Visualization, pages 101–146. Springer Berlin Heidelberg.
- [Schröder and Sweldens, 1995] Schröder, P. and Sweldens, W. (1995). Spherical wavelets: efficiently representing functions on the sphere. In *Proceedings of the 22nd annual conference on Computer graphics and interactive techniques*, SIGGRAPH '95, pages 161–172, New York, NY, USA. ACM.
- [Simoens and Vandewalle, 2003] Simoens, J. and Vandewalle, S. (2003). A stabilized lifting construction of wavelets on irregular meshes on the interval. *SIAM Journal on Scientific Computing*, 24(4):1356–1378.
- [Sweldens, 1998] Sweldens, W. (1998). The lifting scheme: a construction of second generation wavelets. *SIAM J. Math. Anal.*, 29(2):511–546.
- [Sweldens and Schröder, 1996] Sweldens, W. and Schröder, P. (1996). Building your own wavelets at home. In *Wavelets in Computer Graphics, ACM SIGGRAPH Course Notes*.
- [Černá and Finěk, 2011] Černá, D. and Finěk, V. (2011). Construction of optimally conditioned cubic spline wavelets on the interval. *Advances in Computational Mathematics*, 34(2):219–252.